Featured in Physics

Geometric and Conventional Contribution to the Superfluid Weight in Twisted Bilayer Graphene

Xiang Hu,[1,*] Timo Hyart,[2] Dmitry I. Pikulin,[3] and Enrico Rossi[1]
[1]Department of Physics, William & Mary, Williamsburg, Virginia 23187, USA
[2]International Research Centre MagTop, Institute of Physics, Polish Academy of Sciences, Aleja Lotnikow 32/46, PL-02668 Warsaw, Poland
[3]Microsoft Quantum, Microsoft Station Q, University of California, Santa Barbara, California 93106-6105, USA

(Received 20 June 2019; revised manuscript received 11 October 2019; published 5 December 2019)

By tuning the angle between graphene layers to specific "magic angles" the lowest energy bands of twisted bilayer graphene (TBLG) can be made flat. The flat nature of the bands favors the formation of collective ground states and, in particular, TBLG has been shown to support superconductivity. When the energy bands participating in the superconductivity are well isolated, the superfluid weight scales inversely with the effective mass of such bands. For flat band systems one would therefore conclude that even if superconducting pairing is present, most of the signatures of the superconducting state should be absent. This conclusion is at odds with the experimental observations for TBLG. We calculate the superfluid weight for TBLG taking into account both the conventional contribution and the contribution arising from the quantum geometry of the bands. We find that both contributions are larger than one would expect treating the bands as well isolated, that at the magic angle the geometric contribution is larger than the conventional one, and that for small deviations away from the magic angle the conventional contribution is larger than the geometric one. Our results show that, despite the flatness of the bands the superfluid weight in TBLG is finite and consistent with experimental observations. We also show how the superfluid weight can be tuned by varying the chemical potential and the twist angle opening the possibility to tune the nature of the superconducting transition between the standard BCS transition and the Berezinskii-Kosterlitz-Thouless transition.

DOI: 10.1103/PhysRevLett.123.237002

The ability to control accurately the twist angle θ between two-dimensional crystals forming a van der Waals systems [1–4] has recently emerged as a powerful way to tune the electronic properties of a condensed matter system. The most remarkable example of such tunability has been observed in twisted bilayer graphene (TBLG). For most values of the twist angle between the graphene sheets, the systems behave as a normal two-dimensional (2D) semimetal; however, for specific "magic angles" [5–9] the system's lowest energy bands become almost completely flat and the system may support topological properties [10–14]. Quenched kinetic energy in the flat bands increases the importance of interactions and leads to superconductivity and other correlated states [15–27] recently observed in graphene moiré superlattices [28–37]. The hallmark signature of the superconducting state is the absence of electrical resistance. For this to happen the superfluid weight D^s_{xx} must be nonzero. For an isolated parabolic band at zero temperature, $D^s_{xx} \propto n/m^*$, where n is the electron density and m^* the effective electron's mass. From this expression one would conclude that the standard signature of superconductivity might be absent for flat bands because one expects $1/m^*$ to vanish proportionally to the bandwidth. This is not what happens experimentally in TBLG.

In order to reconcile experimental observations and theory, we notice that the above expression for D^s_{xx} assumes an isolated band and neglects the interband matrix elements of the current operator. Neither of these assumptions is valid in TBLG. In an isolated band the density of electrons within the band is constant, and therefore when the superconducting transition occurs, the chemical potential is renormalized. The superfluid weight depends strongly on the chemical potential, and this renormalization is responsible for the appearance $1/m^*$ dependence of the intraband (conventional) contribution to the superfluid weight. In a semimetal where both electron- and holelike bands are present, such as TBLG, the densities in each band are not conserved in the transition separately and the dependence on the chemical potential is weak so that the conventional contribution can be much larger than expected for isolated bands. Moreover, the bandwidth of the low-energy bands, even though very small, is still finite and larger than the superconducting gap. Therefore, the velocity can be large at some points of the Brillouin zone (BZ), further enhancing the conventional contribution to the weight. On the other hand, the interband matrix elements give rise to the so-called geometric part of D^s_{xx}, which can be large even for completely flat band well isolated from other bands [38,39].

In this work we calculate the superfluid weight of superconducting twisted bilayer graphene taking into account both the conventional and the geometric parts. We assume singlet pairing and use the experimentally measured value of T_c to set the value of the coupling constant that enters the mean field gap equation. We obtain the dependence of the superconducting weight on the twist angle and separate the conventional and geometric parts. We find that at one of the magic angles, $\theta = 1.05°$, the geometric contribution is approximately twice as large as the conventional one. However, just off the magic angle the conventional contribution is larger than the geometric one. We also obtain the dependence of the Berezinski-Kosterlitz-Thouless (BKT) T_{KT} temperature on θ and show that its scaling with the chemical potential is different at the magic angle and away from it. Because our calculations take into account the full band structure of TBLG and include both intra- and interband contributions, they can be used for quantitative predictions and they go beyond the models and approximations previously used in deriving bounds for the superfluid weight [40,41].

To model the TBLG we use the approach described in Refs. [8,17]. The low-energy states of the isolated single layers of graphene are located at the $\mathbf{K}$ and $\mathbf{K}' = -\mathbf{K}$ valleys of the BZ. Close to $\mathbf{K}$ the Hamiltonian for each layer $l = \pm 1$ is

$$H_{\mathbf{K},l}(\mathbf{k}) = e^{-il(\theta/4)\tau_z}[\hbar v_F(\mathbf{k} - \boldsymbol{\kappa}_l)\cdot\boldsymbol{\tau} - \mu\tau_0]e^{il(\theta/4)\tau_z}, \quad (1)$$

where $v_F = 10^6$ m/s is graphene's Fermi velocity, μ is the chemical potential, and τ_i ($i = 0, 1, 2, 3$) are the 2×2 Pauli matrices in sublattice space. Because of the rotation of each layer by angle $\theta/2$, the Dirac cone position in layer l is shifted to $\boldsymbol{\kappa}_l$. We choose moiré BZ in which $\boldsymbol{\kappa}_l$ are located at the corners and refer to the center of this BZ as the γ point. This leads to a Hamiltonian for TBLG around the $\mathbf{K}$ point,

$$H_{\mathrm{TBLG},\mathbf{K}} = \begin{pmatrix} H_{\mathbf{K},+1} & T(\mathbf{r}) \\ T^\dagger(\mathbf{r}) & H_{\mathbf{K},-1} \end{pmatrix}, \quad (2)$$

with periodically varying interlayer tunneling terms $T(\mathbf{r}) = w[T_0 + e^{-i\mathbf{b}_2\cdot\mathbf{r}}T_{+1} + e^{-i(\mathbf{b}_2-\mathbf{b}_1)\cdot\mathbf{r}}T_{-1}]$, where $T_j = \tau_0 + \cos(2\pi j/3)\tau_x + \sin(2\pi j/3)\tau_y$, $\mathbf{b}_1 = (\sqrt{3}Q, 0)$ and $\mathbf{b}_2 = (\sqrt{3}Q/2, 3Q/2)$ are reciprocal basis vectors, $Q = (8\pi/3a_0)\sin(\theta/2)$, a_0 is the lattice constant of graphene, and $w = 118$ meV [17,42]. $H_{\mathbf{K}'}$ is obtained from $H_{\mathbf{K}}$ via time reversal.

We leave d-wave pairing [17] for future studies and focus on s-wave pairing. In the presence of superconductivity the mean field theory in Nambu space is described by the Bogoliubov–de Gennes Hamiltonian,

$$H_{\mathrm{BdG}} = \begin{bmatrix} H_{\mathrm{TBLG},\mathbf{K}}(\mathbf{k}) & \hat{\Delta}_s \\ \hat{\Delta}_s^\dagger & -H^T_{\mathrm{TBLG},\mathbf{K}'}(-\mathbf{k}) \end{bmatrix}, \quad (3)$$

and $\hat{\Delta}_s = \Delta\tau_0\sum_{\mathbf{b}}\Delta_{\mathbf{b}}e^{i\mathbf{b}\cdot\mathbf{r}}$, where Δ is the overall amplitude of the superconducting gap, and $\Delta_{\mathbf{b}}$ is the normalized coefficient of the $\mathbf{b} = m_1\mathbf{b}_1 + m_2\mathbf{b}_2$ ($m_i \in Z$) Fourier component. In the remainder of the Letter, we assume $\Delta = 1.764k_BT_c$ and determine T_c and the coefficients $\Delta_{\mathbf{b}}$ by solving the linearized gap equation [17,43].

Using standard linear response theory we can obtain the expression for the superconducting weight [38,39,43],

$$D^s_{\mu\nu} = \sum_{\mathbf{k},i,j}\frac{n(E_j) - n(E_i)}{E_i - E_j}\left(\frac{1}{4L^2}\langle\psi_i|\hat{v}_\mu|\psi_j\rangle\langle\psi_j|\hat{v}_\nu|\psi_i\rangle - \frac{1}{L^2}\langle\psi_i|\hat{v}_{cf,\mu}|\psi_j\rangle\langle\psi_j|\hat{v}_{cf,\nu}|\psi_i\rangle\right), \quad (4)$$

where $L\times L$ is the size of the two-dimensional system, $n(E)$ is the Fermi distribution function, E_i, $|\psi_i(\mathbf{k})\rangle$ are the eigenvalues and eigenvectors of H_{BdG}, and $\mu, \nu = x, y$ represent the directions. In the remainder of the Letter, we focus on the case $\nu = \mu$. We have the velocity operators $\hat{v}_\mu(\mathbf{k}) = \partial H_{\mathrm{BdG}}/\partial k_\mu$, $\hat{v}_{cf,\mu}(\mathbf{k}) = (1/2)\gamma_z\partial H_{\mathrm{BdG}}/\partial k_\mu$ (γ_z is the Pauli matrix acting in Nambu space).

Let H_+ and H_- be the particle and hole Hamiltonians, respectively, of H_{BdG}, $|\psi_{\pm m}\rangle$ the eigenstates of $H_\pm$, $w_{\pm im} \equiv \langle\psi_{\pm m}|\psi_i\rangle$, and $v^+_\mu \equiv \partial_\mu H_+$, $v^-_\mu \equiv -\partial_\mu H_-$. In terms of these quantities, we have [39]

$$D^s_{\mu\mu} = \frac{1}{L^2}\sum_{\mathbf{k}ijmnpq}\frac{n(E_i) - n(E_j)}{E_i - E_j} w^*_{+im}v^+_{\mu mn}w_{+jn}w^*_{-jp}v^-_{\mu pq}w_{-iq}, \quad (5)$$

where m, n and p, q index the particle and hole bands. The matrix elements with $m \neq n$ and $p \neq q$ in Eq. (5) represent pure interband contribution. By defining

$$V^d_{\pm\mu ij} \equiv \sum_m w^*_{\pm im}v^\pm_{\mu mm}w_{\pm jm},$$
$$V^o_{\pm\mu ij} \equiv \sum_{m\neq n} w^*_{\pm im}v^\pm_{\mu mn}w_{\pm jn},$$

we can separate Eq. (5) into a conventional and a geometric part:

$$D^{s,\mathrm{conv}}_{\mu\mu} = \frac{1}{L^2}\sum_{\mathbf{k}ij}\frac{n(E_i) - n(E_j)}{E_i - E_j}(V^d_{+\mu ij}V^d_{-\mu ji} + V^d_{+\mu ij}V^o_{-\mu ji} + V^o_{+\mu ij}V^d_{-\mu ji}),$$
$$D^{s,\mathrm{geom}}_{\mu\mu} = \frac{1}{L^2}\sum_{\mathbf{k}ij}\frac{n(E_i) - n(E_j)}{E_i - E_j}V^o_{+\mu ij}V^o_{-\mu ji}. \quad (6)$$

Below we show that both the conventional [44,45] and the geometric contribution [38,39] are important for the superfluid weight in TBLG.

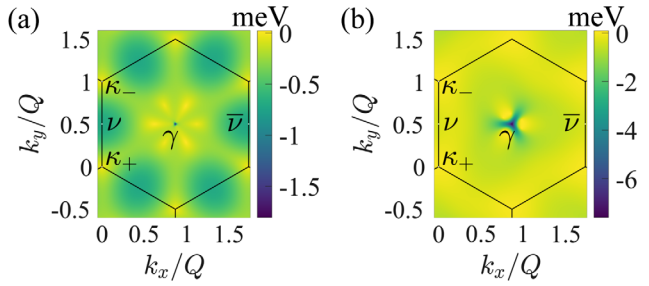

FIG. 1. The dispersion of the lower flat band of TBLG for (a) $\theta = 1.05°$ and (b) $\theta = 1.00°$. The high symmetric points in the moiré BZ are also shown.

Figure 1 shows the dispersion of the lower flat band without superconductivity. It is plotted in the moiré BZ for two different values of θ: $\theta = 1.05°$, the magic angle, and $\theta = 1.00°$. For each angle we see a sharp feature in the dispersion at the γ point, which is away from zero energy. For $\theta = 1.05°$, the bandwidth of the nearly flat moiré band is about 2 meV, whereas for $\theta = 1.00°$ it is around 5 meV. The bandwidth of the lowest energy bands and the value of the magic angle can differ between experiments [46], a fact that can be taken into account by tuning w; see Ref. [43]. For $\theta = 1.00°$, we see that the bands exhibit deep and narrow valleys; green regions emanating from the γ point. Around these valleys the quasiparticle energy $\epsilon(\mathbf{k})$ varies rapidly with $\mathbf{k}$, producing high local velocity despite the fact that the bandwidth is only few meVs.

Figures 2(a) and 2(b) show the profile of $\epsilon(\mathbf{k})$ for the lowest excitation in the presence of s-wave pairing, for $\theta = 1.05°$ and $\theta = 1.00°$. The amplitude and Fourier components of the superconducting gap are obtained by solving the mean field gap equation [43]. We see that also in the presence of a superconducting gap the bands exhibit the same qualitative features as the bands with no pairing, Fig. 1.

Figures 2(c) and 2(d) show the momentum space profile of the integrand, $d_{xx}^{\mathrm{s,conv}}(\mathbf{k})$, that enters the expression (6) for $D_{xx}^{\mathrm{s,conv}}$ for $\theta = 1.05°, 1.00°$, respectively. We see that for $\theta = 1.05°$, $d_{xx}^{\mathrm{s,conv}}$ is peaked at the γ point, and is otherwise quite uniform and small. At bands crossings $d_{xx}^{s,\mathrm{geom}}$ is expected to be large as long as the Berry curvature is not zero, regardless of the nature of the crossing [47]. For $\theta = 1.00°$, $d_{xx}^{\mathrm{s,conv}}$ is strongly peaked at the position of the valleys that we identified in Fig. 1(b). This clearly shows that the conventional contribution to D^s can depend very strongly on the twist angle and in general cannot be assumed to be negligible despite the smallness of the bandwidth. The reason is that even for narrow bands, the expectation value of the velocity operators can be non-negligible. Figures 2(e) and 2(f) show the profile of the integrand, $d_{xx}^{\mathrm{s,geom}}(\mathbf{k})$, that enters the expression of $D_{xx}^{\mathrm{s,geom}}$ for the same conditions used to obtain Figs. 2(c) and 2(d). For $\theta = 1.05°$, $d_{xx}^{\mathrm{s,geom}}(\mathbf{k})$ is strongly peaked at the γ point and on average is larger than the conventional term.

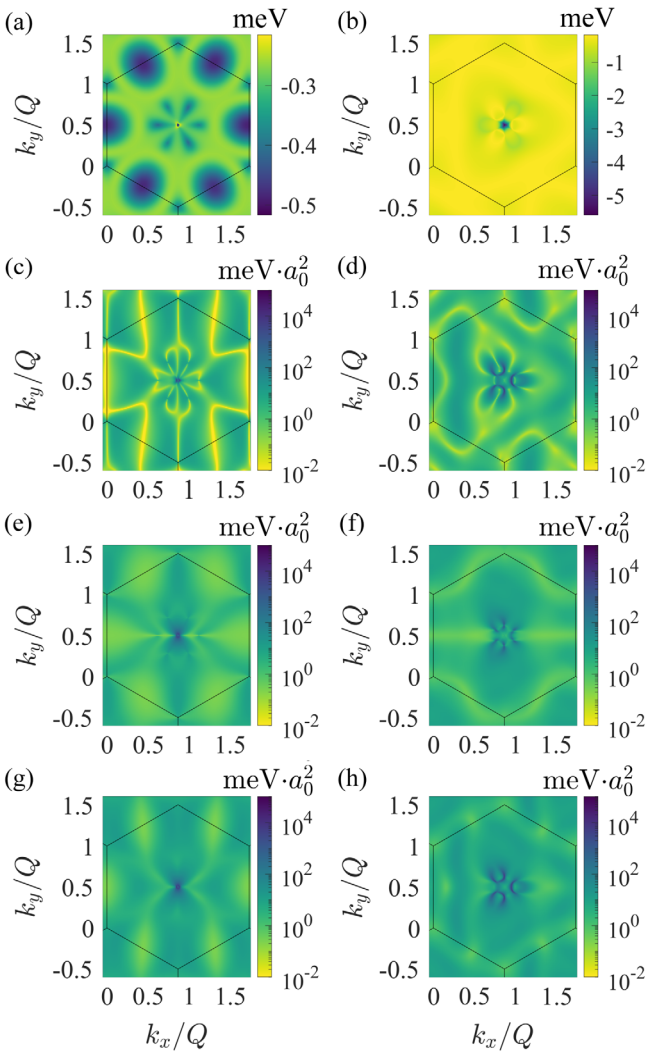

FIG. 2. The dispersion of superconducting band and superfluid weight integrand. Left-hand column, $\theta = 1.05°$; right-hand column, $\theta = 1.00°$. (a),(b) The lowest quasiparticle bands with superconducting gap. (c),(d) $d_{xx}^{\mathrm{s,conv}}(\mathbf{k})$. (e),(f) $d_{xx}^{\mathrm{s,geom}}(\mathbf{k})$. (g), (h) $d_{xx}^{s,\mathrm{total}}(\mathbf{k})$. All the figures are obtained with $\mu = -0.30$ meV and $T_c = 1.6305$ K, $T_c = 1.2119$ K for $\theta = 1.05°$, $\theta = 1.00°$, respectively.

This shows that at the magic angle the geometric contribution to D_{xx}^s is significant and larger than the conventional contribution. For $\theta = 1.00°$, however, $d_{xx}^{\mathrm{s,conv}}(\mathbf{k})$ is large in most of the moiré BZ so that the conventional contribution to D_{xx}^s is larger than the geometric one. As the bands become flatter, the conventional contribution, for fixed electron's density, decreases and so we can expect its importance to decrease relative to the geometric contribution. Figures 2(g) and 2(h) show the sum $d_{xx}^{\mathrm{s,conv}}(\mathbf{k}) + d_{xx}^{\mathrm{s,geom}}(\mathbf{k})$. It is worth pointing out that the spin Chern number C of the lowest energy bands is zero, but in general $D_{xx}^{\mathrm{s,geom}}$ is nonzero even when $C = 0$ [39].

We continue by obtaining the dependence of $D_{xx}^{\mathrm{s,conv}}$ and $D_{xx}^{\mathrm{s,geom}}$ on the chemical potential. From the initial

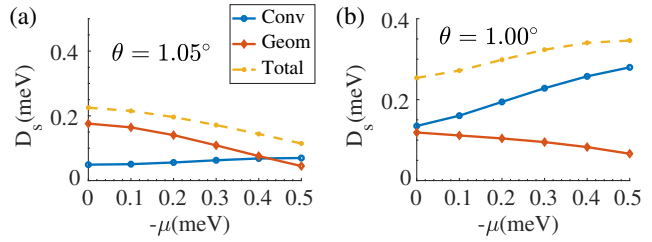

FIG. 3. D_s as a function of the chemical potential for (a) $\theta = 1.05°$ and (b) $\theta = 1.00°$ at $\Delta = \Delta(\mu)$.

discussion we expect $D_{xx}^{\mathrm{s,conv}}$ to increase with the electron density and therefore with $|\mu|$. The scaling of $D_{xx}^{\mathrm{s,geom}}$ with respect to μ depends on the details of the quantum metric of the bands [39]. Figure 3 shows the evolution of $D_{xx}^{\mathrm{s,conv}}$, $D_{xx}^{\mathrm{s,geom}}$, and D_{xx}^{s} with μ for the cases of $\theta = 1.05°$ and $\theta = 1.00°$. To obtain these results the superconducting gap is obtained for each value of μ. The results of Fig. 3 confirm the expectation that $D_{xx}^{\mathrm{s,conv}}$ increases with $|\mu|$, for both the magic angle and $\theta = 1.00°$. They also show that for both angles the geometric contribution decreases with $|\mu|$. Considering that D_{xx}^{s} controls the critical temperature T_{KT} for the Berezinskii-Kosterlitz-Thouless phase transition [48,49], the results of Fig. 3 show that in TBLG it could be possible in principle to tune the nature of the transition, BCS or BKT, by simply varying the doping.

An increase of Δ, keeping μ fixed, is expected to cause an increase of D_{xx}^{s}. This is confirmed by the results of Fig. 4. Again, we can see at $\theta = 1.05°$ the geometric contribution is significant while at $\theta = 1.00°$ the conventional contribution dominates.

In Figs. 5(b) and 5(d) we show the BKT transition temperature as a function of μ obtained from the equation $k_B T_{\mathrm{KT}} = \pi D^s[\Delta(T_{\mathrm{KT}}), T_{\mathrm{KT}}]$, assuming $\Delta(T) = 1.764 k_B T_c \sqrt{1 - T/T_c}$. The prefactor on the rhs of the equation for T_{KT} is twice $\pi/2$ due to the valley degeneracy. In Figs. 5(a) and 5(c) the curves with solid circles show the evolution of $D^s[\Delta(T), T]$ with T for different values of μ for $\theta = 1.05°$ and $\theta = 1.00°$, respectively. The intersection of these curves with the solid line $k_B T$ returns the values of $T_{\mathrm{KT}}(\mu)$. We note that T_{KT} is fairly close to T_c, well above the lower bound set by previous studies [41].

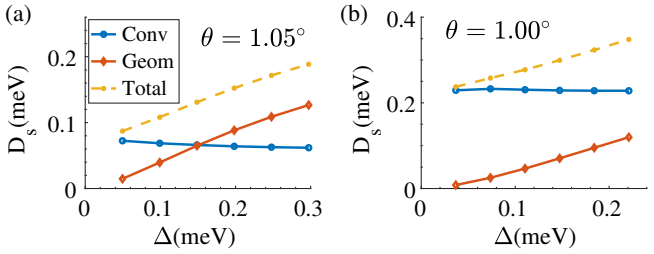

FIG. 4. D_s as a function of Δ for $\theta = 1.05°$ (a) and $\theta = 1.00°$ (b). $\mu = -0.3$ meV.

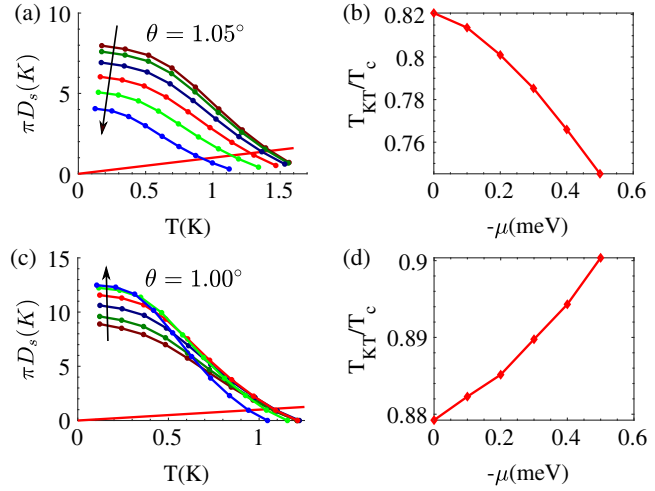

FIG. 5. (a) D^s versus T for $\theta = 1.05°$ and different values of μ: μ goes from 0 to -0.5 meV along the direction of the arrow. (b) T_{KT}/T_c as function of μ for $\theta = 1.05°$. (c) Same as (a) for $\theta = 1.00°$. (d) T_{KT}/T_c as function of μ for $\theta = 1.00°$.

We obtained the value of D_{xx}^{s} ($D_{xx}^{\mathrm{s,conv}}$, $D_{xx}^{\mathrm{s,geom}}$) for different twist angles using the corresponding values of T_c. The results are shown in Fig. 6(a). We see that despite the fact that T_c is lower for $\theta = 1.10°$ than for $\theta = 1.05°$, the superconducting weight is larger for $\theta = 1.10°$. This is because for $\theta = 1.10°$ the conventional contribution to D_{xx}^{s} is much larger than at the magic angle. The results of Figs. 6(a) clearly show that D_{xx}^{s} varies strongly with the twist angle, and that, as a function of θ, the dominant contribution to D_{xx}^{s} can either be the conventional or the geometric one. It is somewhat surprising that even for twist angles as small as 1.00°, corresponding to a bandwidth of the lowest energy bands of just 5 meV, the conventional contribution is larger than the geometric one.

Figure 6(b) shows the dependence of T_c and T_{KT} on the twist angle. We see that both T_c and T_{KT} are maximum at the magic angle and decrease rapidly for θ larger than the magic angle. The results of Fig. 6(b) suggest that it may be possible to tune T_{KT} by tuning the twist angle. Taking into account finite size effects, this can change the nature of the normal-superconductor phase transition.

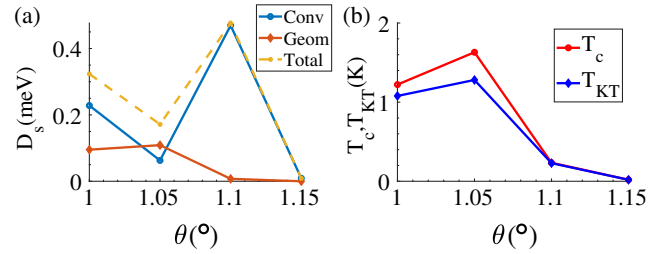

FIG. 6. (a) D_s and (b) T_c and T_{KT} as functions of twist angle. $\mu = -0.3$ meV.

In summary, we have shown that in twisted bilayer graphene, despite the flatness of the low-energy bands, the superconducting weight D^s_{xx} is finite and large enough to explain the experimental observation of superconducting behavior in these systems. We find that the share of the geometric and conventional contributions to D^s_{xx} depends on the twist angle: at the magic angle the geometric contribution dominates, while for angles slightly away from the magic angle the conventional contribution dominates. This qualitative difference is also reflected in the scaling of D^s_{xx} with μ: at the magic angle D^s_{xx} decreases with $|\mu|$, a somewhat surprising result due to the conventional contribution to D^s_{xx} being almost independent of μ, whereas the geometric, large, contribution decreases with $|\mu|$ at the magic angle. Away from the magic angle we find the more conventional behavior of D^s_{xx} growing with $|\mu|$ as the conventional contribution, that grows with $|\mu|$, dominates. This has the important implication that at the magic angle, by simply increasing $|\mu|$ twisted bilayer graphene can be tuned into a regime for which the Berezinzki-Kosterlits-Thouless transition is significantly smaller than the BCS critical temperature. This result shows that twisted bilayer graphene is an exceptional system in which the nature, BKT or BCS, of the superconducting transition can be tuned and experimentally studied in unprecedented ways. We stress that the superfluid weight is one of the few observable signatures of the Berry phase in the Brillouin zone. Measurements of the superfluid weight with the known experimental techniques [50–54] can directly test our predictions of its parametric dependencies.

X. H. and E. R. acknowledge support from NSF (CAREER Grant No. DMR-1455233) and ONR (Grant No. ONR-N00014-16-1-3158). E. R. also acknowledges support from ARO (Grant No. W911NF-18-1-0290). E. R. also thanks the Aspen Center for Physics, which is supported by National Science Foundation Grant No. PHY-1607611, where part of this work was performed. The numerical calculations have been performed on computing facilities at William & Mary, which were provided by contributions from the NSF, the Commonwealth of Virginia Equipment Trust Fund, and ONR. T. H. was supported by the Foundation for Polish Science through the IRA Programme co-financed by EU within SG OP.

Note added.—Recently, we became aware of a related recent preprint by A. Julku *et al.* [55].

*phyxiang@gmail.com

[1] G. Li, A. Luican, J. M. B. Lopes dos Santos, A. H. Castro Neto, A. Reina, J. Kong, and E. Y. Andrei, Nat. Phys. **6**, 109 (2010).
[2] A. K. Geim and I. V. Grigorieva, Nature (London) **499**, 419 (2013).
[3] K. S. Novoselov, A. Mishchenko, A. Carvalho, and A. H. C. Neto, Science **353**, aac9439 (2016).
[4] P. Ajayan, P. Kim, and K. Banerjee, Phys. Today **69**, No. 9, 38 (2016).
[5] J. M. B. Lopes dos Santos, N. M. R. Peres, and A. H. Castro Neto, Phys. Rev. Lett. **99**, 256802 (2007).
[6] E. J. Mele, Phys. Rev. B **81**, 161405(R) (2010).
[7] E. Suarez Morell, J. D. Correa, P. Vargas, M. Pacheco, and Z. Barticevic, Phys. Rev. B **82**, 121407(R) (2010).
[8] R. Bistritzer and A. H. MacDonald, Proc. Natl. Acad. Sci. U.S.A. **108**, 12233 (2011).
[9] G. Trambly de Laissardière, D. Mayou, and L. Magaud, Phys. Rev. B **86**, 125413 (2012).
[10] Z. Song, Z. Wang, W. Shi, G. Li, C. Fang, and B. A. Bernevig, Phys. Rev. Lett. **123**, 036401 (2019).
[11] B. Lian, F. Xie, and B. A. Bernevig, arXiv:1811.11786.
[12] H. C. Po, L. Zou, T. Senthil, and A. Vishwanath, Phys. Rev. B **99**, 195455 (2019).
[13] J. Liu, J. Liu, and X. Dai, Phys. Rev. B **99**, 155415 (2019).
[14] J. Ahn, S. Park, and B.-J. Yang, Phys. Rev. X **9**, 021013 (2019).
[15] N. B. Kopnin, T. T. Heikkilä, and G. E. Volovik, Phys. Rev. B **83**, 220503(R) (2011).
[16] R. Ojajärvi, T. Hyart, M. A. Silaev, and T. T. Heikkilä, Phys. Rev. B **98**, 054515 (2018).
[17] F. Wu, A. H. MacDonald, and I. Martin, Phys. Rev. Lett. **121**, 257001 (2018).
[18] T. J. Peltonen, R. Ojajärvi, and T. T. Heikkilä, Phys. Rev. B **98**, 220504(R) (2018).
[19] H. Guo, X. Zhu, S. Feng, and R. T. Scalettar, Phys. Rev. B **97**, 235453 (2018).
[20] C.-C. Liu, L.-D. Zhang, W.-Q. Chen, and F. Yang, Phys. Rev. Lett. **121**, 217001 (2018).
[21] Y.-Z. You and A. Vishwanath, npj Quantum Mater. **4**, 16 (2019).
[22] Y.-H. Zhang and T. Senthil, Phys. Rev. B **99**, 205150 (2019).
[23] Q.-K. Tang, L. Yang, D. Wang, F.-C. Zhang, and Q.-H. Wang, Phys. Rev. B **99**, 094521 (2019).
[24] B. Roy and V. Juričić, Phys. Rev. B **99**, 121407(R) (2019).
[25] V. Kozii, H. Isobe, J. W. F. Venderbos, and L. Fu, Phys. Rev. B **99**, 144507 (2019).
[26] F. Wu, Phys. Rev. B **99**, 195114 (2019).
[27] F. Wu, E. Hwang, and S. Das Sarma, Phys. Rev. B **99**, 165112 (2019).
[28] K. Kim, A. Dasilva, S. Huang, B. Fallahazad, S. Larentis, T. Taniguchi, K. Watanabe, B. J. LeRoy, A. H. MacDonald, and E. Tutuc, Proc. Natl. Acad. Sci. U.S.A. **114**, 3364 (2017).
[29] Y. Cao, V. Fatemi, S. Fang, K. Watanabe, T. Taniguchi, E. Kaxiras, and P. Jarillo-Herrero, Nature (London) **556**, 43 (2018).
[30] Y. Cao, V. Fatemi, A. Demir, S. Fang, S. L. Tomarken, J. Y. Luo, J. D. Sanchez-Yamagishi, K. Watanabe, T. Taniguchi, E. Kaxiras, R. C. Ashoori, and P. Jarillo-Herrero, Nature (London) **556**, 80 (2018).
[31] M. Yankowitz, S. Chen, H. Polshyn, Y. Zhang, K. Watanabe, T. Taniguchi, D. Graf, A. F. Young, and C. R. Dean, Science **363**, 1059 (2019).
[32] G. Chen, A. L. Sharpe, P. Gallagher, I. T. Rosen, E. J. Fox, L. Jiang, B. Lyu, H. Li, K. Watanabe, T. Taniguchi, J. Jung, Z. Shi, D. Goldhaber-Gordon, Y. Zhang, and F. Wang, Nature (London) **572**, 215 (2019).

[33] X. Lu, P. Stepanov, W. Yang, M. Xie, M. A. Aamir, I. Das, C. Urgell, K. Watanabe, T. Taniguchi, G. Zhang, A. Bachtold, A. H. MacDonald, and D. K. Efetov, Nature (London) **574**, 653 (2019).
[34] C. Shen, N. Li, S. Wang, Y. Zhao, J. Tang, J. Liu, J. Tian, Y. Chu, K. Watanabe, T. Taniguchi, R. Yang, Z. Y. Meng, D. Shi, and G. Zhang, arXiv:1903.06952.
[35] X. Liu, Z. Hao, E. Khalaf, J. Y. Lee, K. Watanabe, T. Taniguchi, A. Vishwanath, and P. Kim, arXiv:1903.08130.
[36] Y. Cao, D. Rodan-Legrain, O. Rubies-Bigordà, J. M. Park, K. Watanabe, T. Taniguchi, and P. Jarillo-Herrero, arXiv:1903.08596.
[37] G. Chen, A. L. Sharpe, E. J. Fox, Y.-H. Zhang, S. Wang, L. Jiang, B. Lyu, H. Li, K. Watanabe, T. Taniguchi, Z. Shi, T. Senthil, D. Goldhaber-Gordon, Y. Zhang, and F. Wang, arXiv:1905.06535.
[38] S. Peotta and P. Törmä, Nat. Commun. **6**, 8944 (2015).
[39] L. Liang, T. I. Vanhala, S. Peotta, T. Siro, A. Harju, and P. Törmä, Phys. Rev. B **95**, 024515 (2017).
[40] T. Hazra, N. Verma, and M. Randeria, Phys. Rev. X **9**, 031049 (2019).
[41] F. Xie, Z. Song, B. Lian, and B. A. Bernevig, arXiv:1906.02213.
[42] J. Jung, A. Raoux, Z. Qiao, and A. H. MacDonald, Phys. Rev. B **89**, 205414 (2014).
[43] See Supplemental Material at http://link.aps.org/supplemental/10.1103/PhysRevLett.123.237002 for more details.
[44] D. J. Scalapino, S. R. White, and S. C. Zhang, Phys. Rev. Lett. **68**, 2830 (1992).
[45] D. J. Scalapino, S. R. White, and S. Zhang, Phys. Rev. B **47**, 7995 (1993).
[46] A. Kerelsky, L. J. McGilly, D. M. Kennes, L. Xian, M. Yankowitz, S. Chen, K. Watanabe, T. Taniguchi, J. Hone, C. Dean, A. Rubio, and A. N. Pasupathy, Nature (London) **572**, 95 (2019).
[47] J.-W. Rhim and B.-J. Yang, Phys. Rev. B **99**, 045107 (2019).
[48] V. L. Berezinskiĭ, Zh. Eksp. Teor. Fiz. **59**, 907 (1970) [Sov. J. Exp. Theor. Phys. **32**, 493 (1971)].
[49] J. M. Kosterlitz and D. J. Thouless, J. Phys. C **6**, 1181 (1973).
[50] A. F. Hebard and A. T. Fiory, Phys. Rev. Lett. **44**, 291 (1980).
[51] S. J. Turneaure, T. R. Lemberger, and J. M. Graybeal, Phys. Rev. Lett. **84**, 987 (2000).
[52] J. A. Bert, B. Kalisky, C. Bell, M. Kim, Y. Hikita, H. Y. Hwang, and K. A. Moler, Nat. Phys. **7**, 767 (2011).
[53] J. A. Bert, K. C. Nowack, B. Kalisky, H. Noad, J. R. Kirtley, C. Bell, H. K. Sato, M. Hosoda, Y. Hikita, H. Y. Hwang, and K. A. Moler, Phys. Rev. B **86**, 060503(R) (2012).
[54] I. Kapon, Z. Salman, I. Mangel, T. Prokscha, N. Gavish, and A. Keren, Nat. Commun. **10**, 2463 (2019).
[55] A. Julku, T. J. Peltonen, L. Liang, T. T. Heikkilä, and P. Törmä, arXiv:1906.06313v2.